Selective Reagent Ion-Time of Flight-Mass Spectrometry study of six common monoterpenes

Dušan Materić[1,2*], Matteo Lanza[3], Philipp Sulzer[3], Jens Herbig[3], Dan Bruhn[1,4], Vincent Gauci[1], Nigel Mason[6], Claire Turner[5]

[1] School of Environment, Earth and Ecosystems, The Open University, Walton Hall, Milton Keynes, MK7 6AA, United Kingdom

[2] Institute for Marine and Atmospheric Research, Utrecht University, 3584CC Utrecht, The Netherlands

[3] IONICON Analytik, Eduard-Bodem-Gasse 3, 6020 Innsbruck, Austria

[4] Section of Biology and Environmental Science, Department of Chemistry and Bioscience, Aalborg University, Fredrik Bajers Vej 7H, 9220 Aalborg East, Denmark

[5] School of Life, Health and Chemical Sciences, The Open University, Walton Hall, Milton Keynes, MK7 6AA, United Kingdom

[6] Department of Physical Sciences, The Open University, Walton Hall, Milton Keynes, MK7 6AA, United Kingdom

[*]Corresponding author: dusan.materic@gmail.com, Tel. +31302537758

Abstract

One of the most common volatile organic compounds (VOCs) group is monoterpenes. Monoterpenes share the molecular formula $C_{10}H_{16}$, they are usually cyclic and have a pleasant smell. The most common monoterpenes are limonene (present in citrus fruits) and α-pinene (present in conifers' resin). Different monoterpenes have different chemical, biological and ecological properties thus it is experimentally very important to be able to differentiate between them in real time. Real time instruments such as Proton Transfer Reaction-Time of Flight-Mass Spectrometry (PTR-ToF-MS), offer a real time solution for monoterpene measurement but at the cost of selectivity resulting in all monoterpenes being seen at the same m/z. In this work we used Selective Reagent Ion-Time of Flight-Mass Spectrometry (SRI/PTR-ToF-MS) in order to explore the differences in ion branching when different ionizations (H_3O^+, NO^+ and O_2^+) and different drift tube reduced field energies (E/N) were used. We report a comprehensive ion library with many unique features, characteristic for individual monoterpenes.

Key words: PTR-MS; PTR-ToF-MS; SRI-ToF-MS; SRI-MS; monoterpenes; E/N

Introduction

Monoterpenes are an omnipresent group of compounds emitted by many organisms. They are the key compounds of plant oleoresin directly participating in plant defense mechanism [1,2], they give signals to the insects associated with plants [3,4], give fruity flavor to our food and beverages [5], they are even present in human breath indicating metabolic state of some organs [6], and they affect our climate globally [7,8].

Analytical methods commonly used for monoterpene analysis are divided into two groups: those using Gas Chromatography (GC) to separate compounds present prior to detection (usually by a mass spectrometer) and direct injection mass spectrometry using chemical ionization (CI). GC-methods (especially Gas Chromatography Mass Spectrometry – GC-MS) have high analytical power and are suitable for both quantitative and qualitative analysis, but at the time cost [9]. On the other hand, direct injection mass spectrometry with CI is a way of ionizing species for separation and analysis by mass spectrometry and it is suitable for real time analysis. Here, the most commonly used techniques are: Proton Transfer Reaction Mass Spectrometry (PTR-MS) [10,11] and Selected Ion Flow Tube Mass Spectrometry (SIFT-MS) [12].

Chemical ionization utilizes charged molecules such as H_3O^+, NO^+ and O_2^+ as a means of ionization, rather than conventional 70 V electron impact ionization, resulting in overall lower fragmentation of the compounds [11]. In this way CI based instruments may achieve good sensitivity in real time, but with less compound selectivity. More analytical power in CI methods, yielding compound identification, has been achieved by altering reduced field energy (E/N) in PTR-MS, or by using different reagent ions, in SIFT-MS [10,12].

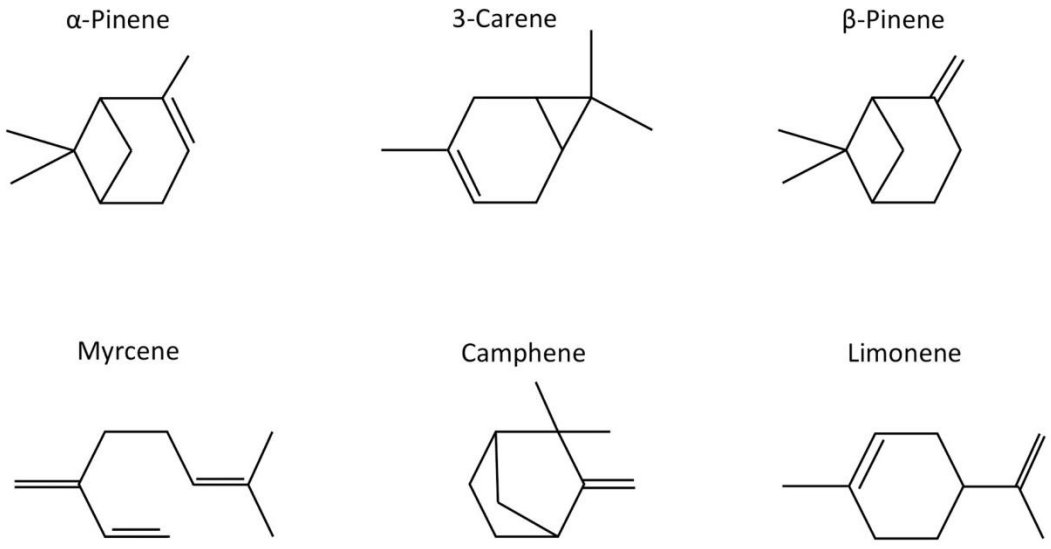

Figure 1. Structure of six monoterpenes investigated in this work

So far, E/N studies with PTR-MS (with limitation to quadrupole instruments and a narrow E/N range) and SIFT-MS measurement (with limitation of quadrupole instrument, low

sensitivity and fixed E/N and) have been used to characterize monoterpenes [13–15]. However, the full potential of SRI-PTR-TOF-MS together with wide E/N range has not yet been explored for many compounds including monoterpenes.

Under standard measurement conditions (E/N 120-140) PTR-MS cannot distinguish different monoterpene isomers as they are predominantly detected at the m/z of the protonated molecule. However, altering the drift tube conditions and utilizing different reagent ions have the analytical potential to resolve monoterpene mixtures. This is of considerable advantage for on-line measurement set-ups, where no time-consuming separation methods can be used.

In this paper fragmentation patterns (branching ratios) of 6 common monoterpenes (Figure 1), using H_3O^+, NO^+, O_2^+ reagent ions and a wide E/N range, are presented in order to provide a comprehensive database of product ion contributions at each condition, in which way more analytical information will be available for potential compound identification.

Materials and methods

Chemicals: The following monoterpene standards have been used for this experiment: (+)-α-pinene (≥98.5%, Fluka), camphene (95%, Sigma Aldrich), (+)-β-pinene (≥98.5%, Fluka), myrcene (≥90%, Sigma Aldrich), (+)-3-carene (≥98.5%, Fluka), and R-(+)-limonene (97%, Sigma Aldrich).

Permeation: In order to provide a stable monoterpene concentration, we used a permeation system. Each sample was loaded onto a 10 cm long polytetrafluoroethylene (PTFE) tube, 6 mm diameter, and sealed with stainless steel caps. Each tube was placed in a glass cylinder capped with a PTFE cap, which had two openings (inlet and outlet) connected to the tubing system. All tubing was made from PTFE and stainless steel. The permeation tube was kept in an oven at 90°C and flushed with a flow of clean air generated from a GCU (IONICON Analytik, Austria). The flow was adjusted from 100 to 500 mL/min in order to provide comparable concentrations for each monoterpene. The overflow was regulated by a needle valve and the flow sent to the instrument was 100 mL/min (see the permeation system diagram in Picture S1). One to three days were required for the system to equilibrate to start the stable permeation process.

PTR-SRI-ToF-MS measurement: The measurement of monoterpene fragmentation was performed using a PTR-TOF 8000 (IONICON Analytik, Austria). We set up an automated measurement containing several steps with different E/N. Starting from E/N = 60 Td, each step was increased by 10 Td, until 240 Td, then decreased back to 60 Td. For each E/N step 20 cycles were performed, 2 s in each cycle, resulting in a total of 40 cycles for each E/N step (20 upstream and 20 downstream, 80 s total measurement time per E/N step). Each monoterpene standard was measured in three ionization modes: H_3O^+, NO^+ and O_2^+ using the same E/N automatization set up.

Data analysis: PTRMS Viewer 3.0 (IONICON Analytik, Austria) was used to identify peaks of interest, to extract the peak data, and for the transmission curve correction. The

transmission curve is determined by analysing a gas standard with compounds spread over a mass range of up to m/z 181 (trichlorobenzene) at standard PTR conditions, as previously shown [16]. The same transition parameters (obtained at standard PTR conditions) have been used for all the E/N measurements as transmission is dependent on the voltages in the transfer system and the ToF, thus not of E/N that we manipulated. Overlapping peaks were separated using "multi-peak" integration (Table S1 – supplementary material), an option available when the user edits the peak data in PTRMS Viewer. We measured a monoterpene fragment at mass m/z 39.0226 using isotope m/z 40.0260 to avoid interference with the isotope of the water cluster $H_2O.H_3O^+$ (m/z 39.0332). Isotope peaks were identified (e.g. m/z 138.1364) and excluded from the analysis, since they provide no additional information. A Perl script has been developed to performed data normalization and averaging. The script normalizes the data to the sum of the following primary ions, including their isotopic correction: (1) H_3O^+ (*m/z* 21.0226), $H_2O.H_3O^+$ (*m/z* 39.0332), and $(H_2O)_2.H_3O^+$ (*m/z* 57.0438) when H_3O^+ is used as reagent ion; (2) m/z 30.9950 + m/z 31.0022 when NO^+ is used as reagent ion and (3) m/z 33.9941 when O_2^+ is used as reagent ion. Exported ions for each monoterpene were normalized to one million of the primary ions (to enable comparability between instruments with different primary ion yields), and figures were generated using SigmaPlot 13.

Impurities exclusion: When the PTR-ToF-MS data obtained using H_3O^+ were analysed we took previously identified monoterpene ions from the literature [13,15,17], made the ion table and extracted these ions (Table S1). We also performed the peak detection with the low threshold in order to identify new peaks. Impurities from the system were excluded by measuring it as a background signal, which we subtracted from the raw signal. Impurities from the standards were excluded by excluding ions containing non monoterpene atoms (e.g. oxygen). Additionally, we used signal intensity threshold levels in accordance with impurities levels below which ions were excluded (e.g. 10% for myrcene). We also excluded commonly known isotopes (e.g. m/z 138).

When NO^+ and O_2^+ data were analysed, no previous PTR-SRI-MS ion information of the monoterpenes was available. First, we obtained peak detection with a low threshold and subtracted the background from the signal, in this way all the impurities from the system were excluded. Second, we identified the chemical formula for each ion detected on the basis of the exact molecular mass (read by high resolution ToF), using the program mMass 5.5 (http://www.mmass.org). Third, we excluded peaks containing non monoterpene atoms and structure (e.g. oxygen). Ions with intensities below a set threshold (according to the impurity levels) were excluded.

Results and discussion

Ion branching ratios for each ionization method are summarized in Figure 2-7. A list of all monoterpene ions produced for each of the analysed monoterpenes is shown in Table S2 – supplementary material. Previous PTR-MS work on monoterpenes employed quadrupole instruments, a narrow range of E/N (80-120 Td), and only four monoterpenes from this study were covered [15,17]. In contrast, we covered a wider E/N range (60-240 Td) and used PTR-ToF-MS, which allowed better resolution and analytical performance.

The most common monoterpene fragments (ions) produced when H_3O^+ is used are recognized to be m/z 137, 135, 121, 119, 109, 107, 95, 93, 81, 79, 67, 57, 41 and 39 [13,15,17] (exact masses for each ion discussed in the text can be found in Table S2). However, some authors consider that standard impurity or equipment material may be the reason for some of the observed ions, but disagree on which ones [13,15]. As these impurities should also be present in our background measurement we excluded equipment material as a possibility. We included all previously observed ions, identified some more, and tentatively attribute them to originating from the monoterpenes. However, a recently developed fastGC-PTR-ToF-MS method may provide a way to experimentally confirm the origin of these monoterpene ions [18].

Apart from ionization with H_3O^+ (proton transfer reaction) we also used more energetic NO^+ and O_2^+ (charged transfer) ionization (SRI-MS) [16,19]. Monoterpene analysis with this novel ionization method of SRI/PTR-TOF-MS has not previously been reported, although some work has been reported using a different chemical ionization based method that does not vary E/N (SIFT-MS) [14]. As expected, relative abundance of molecular ion (m/z 136) using NO^+ and O_2^+ has found at much lower values compare to protonated molecular ions using H_3O^+. However, we observed similar trend that molecular ion abundance decreased when E/N was increasing.

Here we focus on ion branching ratios and ion behaviour with varying E/N for all three ionization modes. Schematics for monoterpene fragmentation and hypotheses on the formation of product ions may be found elsewhere [13,14,17].

Monoterpene reactions with H_3O^+

α-Pinene: The branching ratio of α-pinene, characteristic of all the monoterpenes, showed that the major ions are m/z 137, m/z 91, m/z 81, m/z 79 and m/z 39 (Figure 2a). Other ions contributing more than 5% at any E/N were m/z 95, m/z 93 and m/z 41 (Figure 2b). While the (protonated) molecular ion m/z 137 gradually decreases with higher E/N, ion m/z 81 increases until a critical point (E/N 150 Td) and then decreases. Ion m/z 93 showed a similar pattern change to ion m/z 81 but with an order of magnitude lower contribution. After the critical point of 150 Td, ions m/z 41 and m/z 39 started to increase, and from 190 Td, m/z 39 became the major ion. Ion m/z 92 gradually increases across E/N, but ion m/z 95 has a bell shape with the maximum around E/N 180 Td reaching a relative contribution of 7%.

There is a notable difference in behaviour of two major ions (m/z 137 and 81) during the change of E/N compared to that described in previous work [15,20], in which a quadrupole was used instead of a ToF. In our work, the relative ion abundance of these two ions were equal at 110 Td, which is lower value in respect to the previously published data. Also, the ion m/z 137 started from slightly higher (80 %), and m/z 81 slightly lower relative ion abundance (10 %). This could be explained by (1) data processing, as they might not perform the transmission curve correction and/or (2) differences between quadrupole and ToF instruments (e.g. transmission curve difference). We also measured a slightly higher concentration of m/z 95, and did not observe m/z 67 [15]. We also did not observe ions m/z 109 and m/z 107 as previously reported [17]. However, we discovered previously

unreported ions at m/z 92, m/z 91, m/z 80 and m/z 79. As we used a wide range of E/N in our study, we noted that ions m/z 92, 91, 39, and 41 started to increase after E/N reached 150 Td, which is similar for all monoterpenes.

3-Carene: 3-Carene had a similar ion branching pattern to the α-pinene (Figure 2c and 2d). Notable differences are (1) the contribution of m/z 137 and m/z 81 meeting at E/N 130 while in α-pinene it is around 110 Td; (2) the contribution of m/z 39 does not reach that of α-pinene at high E/N. Also the 3-carene ion m/z 135 has a value >4 % at low E/N (<80 Td), which is unique among monoterpenes analysed here. Another unique property of 3-carene is that the ion m/z 91 is the most abundant ion at high E/N (>220 Td).

Even though 3-carene is one of the most dominant monoterpenes in European boreal forests its ion branching in PTR-ToF-MS has not been investigated [15,21,22]. Apart from the overall ratio difference, we observed similar branching ratio pattern for ions m/z 137, 95 and 81, but we have not observed the ion with m/z 67 [15]. Similarly to previous work on 3-carene and 2-carene we also observed ions m/z 93 (>6%) and 121 (but <1%) [13,17]. The rest of the ions identified in this work (Figure 2, Table S2) and their dependence over E/N range are novel.

β-Pinene: The branching ratio of β-pinene has a similar pattern to the α-pinene (Figure 2e and 2f). Uniquely, m/z 135 has a steady value of >3 % below 130 Td. Also, at high E/N, m/z 95 has a higher value than α-pinene but not as high as 3-carene.

Apart from an overall difference in the major ions ratio mentioned earlier when compared with other works (see α-pinene section), we also observed a slightly higher contribution of m/z 95 compared to α-pinene [17]. We also discovered and characterized new ions (m/z 135, 91, 79, 51, 41 and 39) previously not associated with β-pinene [15,17] (Table S2). Ion m/z 51 has only been found at higher E/N for β-pinene and limonene.

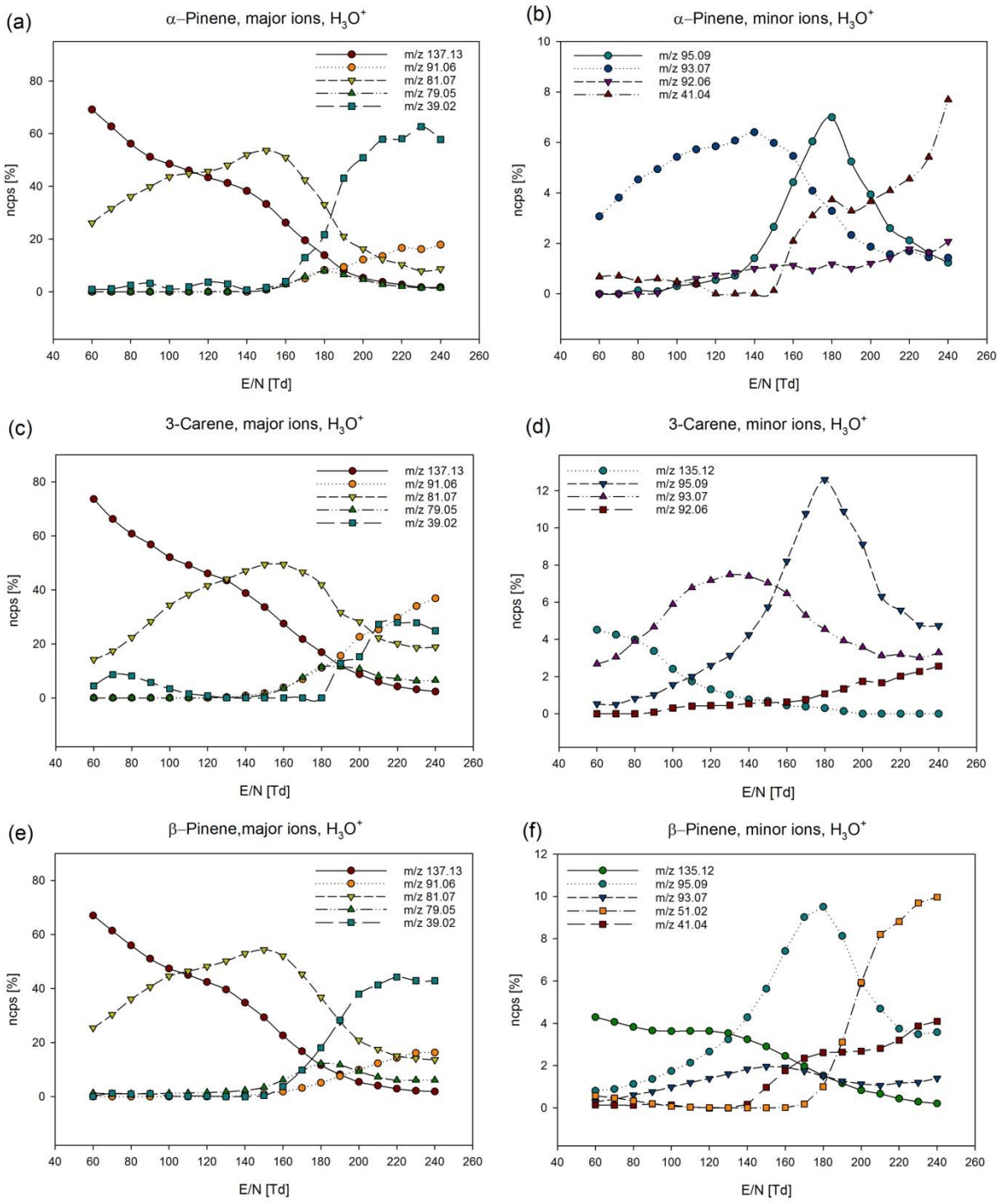

Figure 2. Ion branching of α-pinene, 3-carene and β-pinene using H_3O^+ as reagent ion and E/N 60-240 Td. Note that major ions are left and minor ions right.

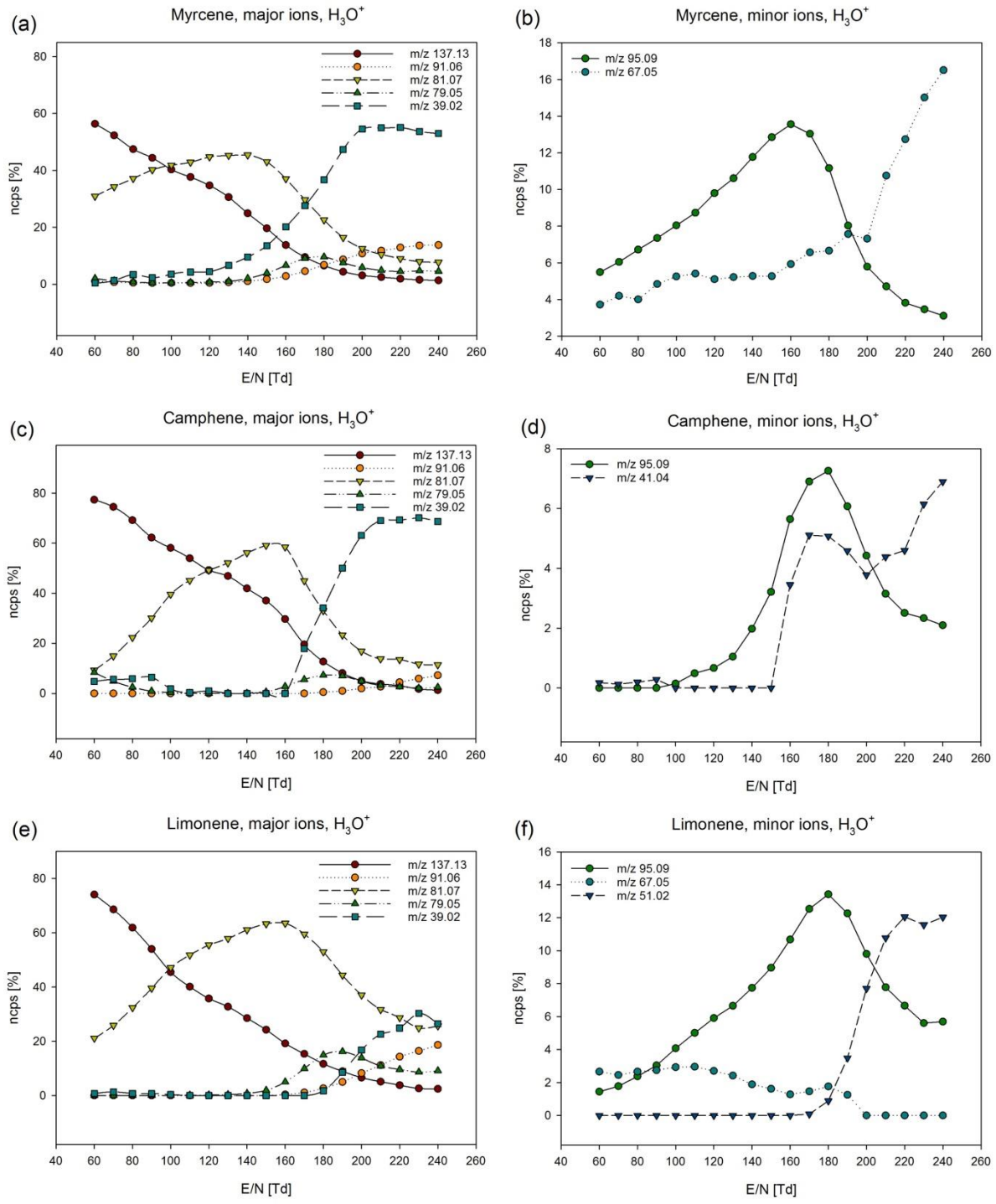

Figure 3. Ion branching of myrcene, camphene and limonene using H_3O^+ as reagent ion and E/N 60-240 Td. Note that major ions are left and minor ions right.

Myrcene: The branching ratio of myrcene has a similar pattern to the α-pinene (Figure 3a and 3b), except that the relative abundance of ions m/z 137 and m/z 81 converge at a lower E/N (100 Td). The unique feature is that the ion m/z 95 has higher relative contribution then α- and β-pinene (>12%), with the maximum E/N not at 180 Td like other monoterpenes, but at 160 Td. Furthermore, the ion m/z 41 suddenly increases at 100 Td and after 130 Td it reaches a plateau with 4% relative ion abundance. We found that ion m/z 69 (contribution of 4% at 100 Td) is a unique property of myrcene amongst the currently studied monoterpenes.

Myrcene has not previously been the focus of study by PTR-MS with E/N shift, so to our knowledge this is the first E/N report of ion branching. Previous measurements obtained at ≈135 Td showed the presence of minor ions m/z 121, 109 and 93 [17]. We also observed these ions, but at intensities below the threshold we set because of potential impurities. Similarly, we also noted a higher concentration of m/z 95 compared to other monoterpenes (Figure 2-3, Table S2). In addition to m/z 137 and m/z 81, ions m/z 95 and m/z 69 have also been observed by SIFT-MS [14].

Camphene: The branching ratios of the ions for camphene show the pattern typical for all monoterpenes (Figure 3c and 3d), with a higher overall contribution of m/z 137, m/z 81 and m/z 39 compare to other monoterpenes. However, uniquely ion m/z 93 slowly increased over the E/N range (Figure 3d). No other ions such as m/z 121, m/z 109 and m/z 107 were observed, in contrast to a previous analysis by quadrupole instrument at ≈135 Td [17]. To our knowledge no E/N study has yet been published for this compound.

R-Limonene: The branching ratio of R-limonene also has a pattern typical for all monoterpenes (Figure 3e and 3f). However we observed a notably higher contribution of the ion m/z 81 compared to m/z 137 at E/N >140 Td. Uniquely, ion m/z 95 had the highest contribution measured in this experiment (13% at 180 Td), and ion m/z 51 behaved with a somewhat similar pattern to that of β-Pinene.

The branching ratio of limonene has been reported previously for E/N 80-170 Td, and only the ions m/z 137, m/z 81 and m/z 67 were observed (not counting the isotopes) [15]. Apart from overall differences in branching ratios obtained by different instruments (explained earlier in the discussion of α-pinene) the similarity with previous data is that the relative ion abundance of m/z 137 and m/z 81 converge earlier E/N compared to 3-carence [15]. We also did not observe m/z 121, which was previously detected at E/N 135 Td [17], however we discovered other ions (Figure 3, Table S2).

Monoterpene reactions with NO^+

α-Pinene: Unlike ionization with H_3O^+, use of NO^+ yields more ions and less mass spectra similarities between monoterpenes. The branching ratio of α-pinene which shares some similarities with all monoterpenes had the following pattern: (1) the most dominant ion at low E/N (<70 Td) was the molecular ion (m/z 136), (2) at 80 to 150 Td the most dominant ion was m/z 92, (3) at E/N >160 ion m/z 91 was dominant, (4) ion m/z 39 started to increase after E/N reached 170 Td (Figure 4a and 4b). While ion m/z 108 was decreasing across E/N,

ions m/z 121 and 94 had a bell shape with peaks at 150 and 120 Td, and ion m/z 77 had a sigmoidal shape. Ion m/z 108 has been noted to be only present for α- and β-pinene.

In previous work with a similar technique only ions m/z 136, m/z 93 and m/z 92 were observed [14], which is similar to the data recorded at low E/N (Figure 4, Table S2).

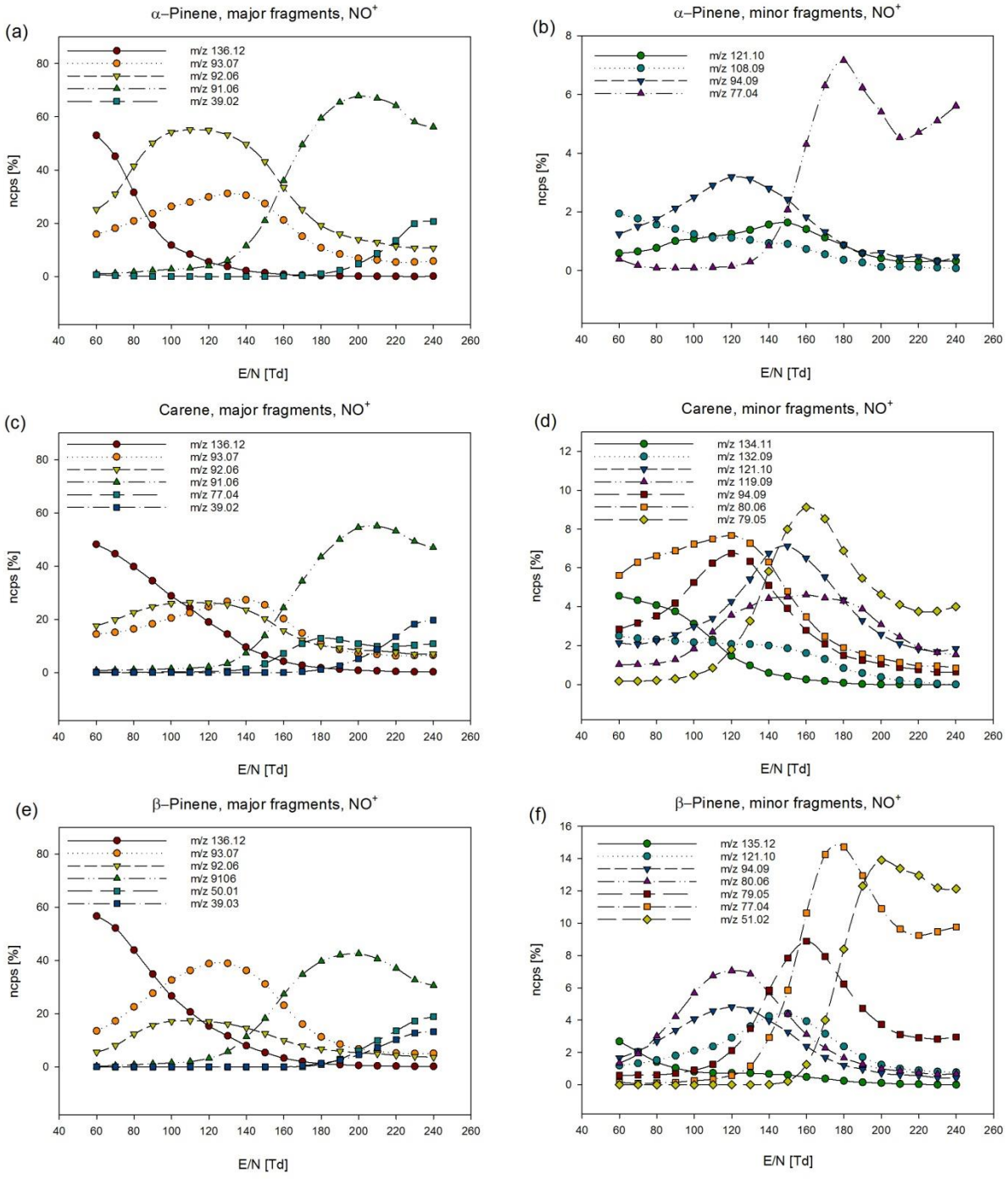

Figure 4. Ion branching of α-pinene, 3-carene and β-pinene using NO^+ as reagent ion and E/N 60-240 Td. Note that major ions are left and minor ions right.

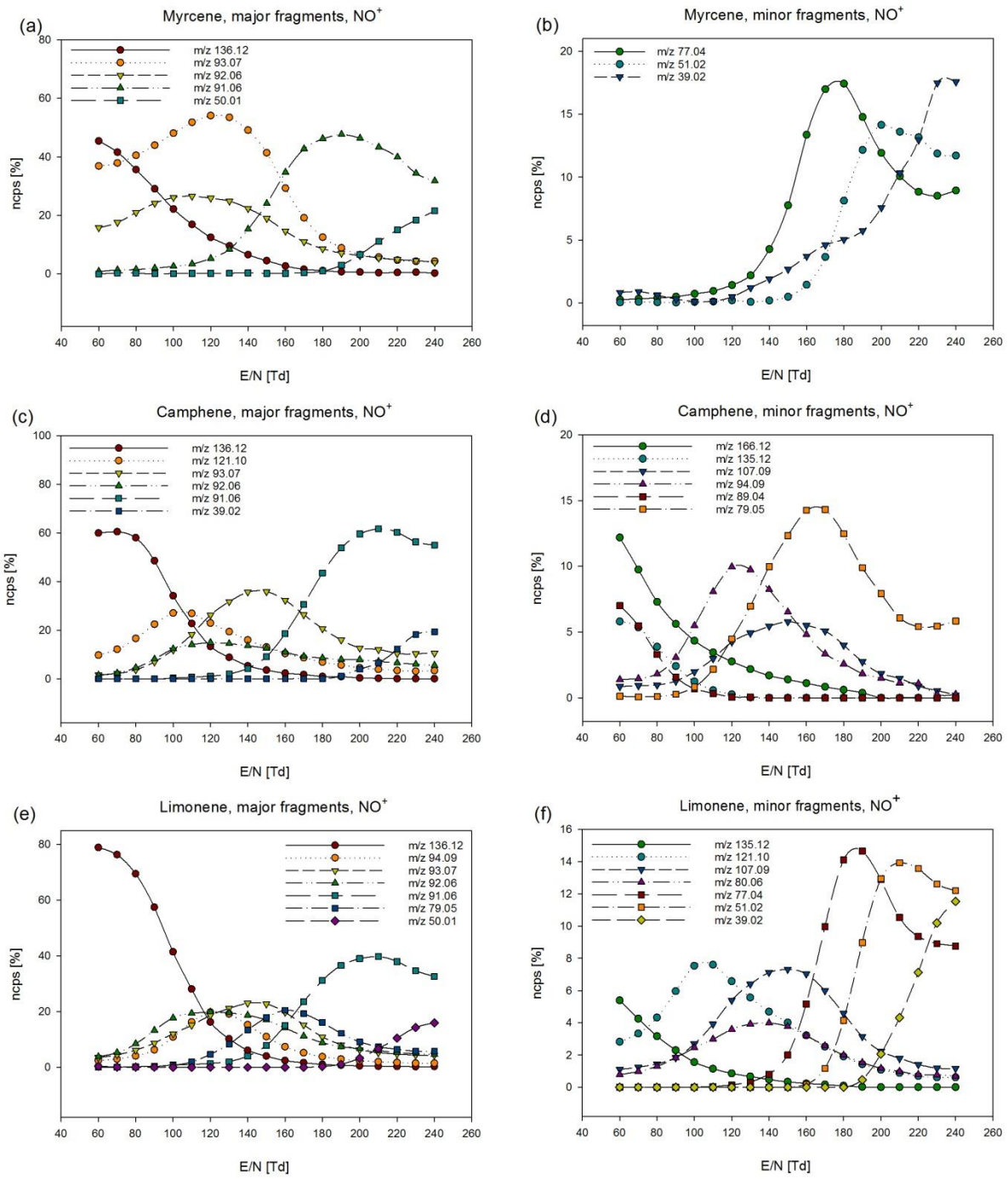

Figure 5. Ion branching of myrcene, camphene and limonene using NO^+ as reagent ion and E/N 60-240 Td. Note that major ions are left and minor ions right.

3-Carene: The branching ratios for 3-carene are shown in Figure 4c and 4d. In contrast to α-pinene the molecular ion m/z 136 dominated at E/N <100 Td, from E/N 110 to 150 Td ions m/z 93 and m/z 92 were the most abundant, and at E/N >160 the ion m/z 91 had the largest relative contribution. Apart from ions m/z 134 and 132, which gradually decreased with an increase of E/N, the rest of the minor ions had a bell shape with the peaks 120 Td (m/z 94 and m/z 80), 130 Td (m/z 121) and 160 Td (m/z 119 and m/z 79). Ion m/z 119 is unique for 3-carene and myrcene, but only 3-carene produces it at higher E/N (>180Td).

In previous work with SIFT-MS only ions m/z 136, m/z 135, m/z 93 and m/z 92 were observed, which is similar to low E/N concentrations of this experiment; however, we did not observe m/z 135 (Figure 4, Table S2) [14].

β-Pinene: The branching ratios of β-pinene are shown in Figure 4e and 4f. Ion m/z 136 dominated at E/N <90, ion m/z 93 between 100 and 150 Td, and ion m/z 91 at E/N >160. A notable difference compared to other monoterpenes (except myrcene) is that at the middle of E/N range (100-150 Td) ion m/z 93 is the most dominant. We also observed adduction ionization with NO^+ that resulted in ions m/z 166, m/z 152, m/z 151 and m/z 150, but only at low E/N and low relative ion abundance. Ion m/z 89 has been exclusively found for β-pinene and camphene, and ions m/z 50 and 51 have been found only for β-pinene, myrcene and limonene.

In previous work with SIFT-MS only the ions m/z 136, m/z 93 and m/z 92 have been observed [14] again, similar to our experiment at low E/N (Figure 4, Table S2). To our knowledge this is the first PTR/SRI-MS β-pinene study using NO^+.

Myrcene: The branching ratios of myrcene are shown in Figure 5a and 5b. At low E/N (<70) the dominant ion was m/z 136, between 80 and 150 Td it was ion m/z 93, and >160 Td it was m/z 91. Similarly to β-pinene, myrcene had a unique signal from ion m/z 93, however it is the most abundant ion at much lower E/N (down to 80 Td).

In previous work with similar technique only ions m/z 136, m/z 93 and m/z 92 have been observed [14], which is similar to the data recorded at low E/N in the present experiment (Figure 5, Table S2).

Camphene: The branching ratios of camphene are shown in Figure 5c and 5d. In common with most monoterpenes, the most abundant ion <100 Td was m/z 136; in the mid E/N range m/z 93 was the dominant ion, and at high E/N (<170 Td) it was ion m/z 91. At E/N 110 Td the most dominant ion was m/z 121, which is unique among analysed monoterpenes. Ion m/z 89, unique for β-pinene and camphene, has been found in higher relative abundances compare to β-pinene. We also observed a high relative abundance of ion m/z 166 at low E/N, formed in adduction ionization with NO^+.

In previous work with SIFT-MS ions m/z 166, m/z 136, m/z 121, m/z 94, m/z 93 and m/z 92 were observed [14], which is similar to the relative abundance of major ions in this experiment at lower E/N (Figure 5, Table S2).

R-Limonene: The branching ratios of limonene share basic similarity to other monoterpenes and it is shown in Figure 5e and 5f. The molecular ion m/z 136 had the highest contribution compared to other monoterpenes at low E/N, and dominated until 110 Td, which is higher

E/N value then compared to other monoterpenes. Between 130 and 150 Td the dominant ion was m/z 93, but at E/N 120 Td m/z 94, m/z 93 and m/z 92 had the similar value of 20 %, which is unique among the current set of monoterpenes. Furthermore, at E/N 160 Td ion m/z 79 was the dominant ion, closely followed by ion m/z 93, this is also a unique feature of limonene. Ions m/z 166, m/z 152, products of adduction ionization with NO^+, were observed but excluded from the plots as they had relative ion abundance <3 % at each E/N.

In previous work with a similar technique only ions m/z 136, m/z 135, m/z 121, m/z 94, m/z 93 and m/z 92 have been observed [14], which once again is similar to the present results at low E/N (Figure 5, Table S2).

Monoterpene reactions with O_2^+

α-Pinene: Unlike H_3O^+ and NO^+ described earlier, ionization with O_2^+ brings stronger fragmentation which yields an almost unrecognizable pattern shared by all monoterpenes analysed here. Accordingly, the branching ratios of each monoterpenes obtained using O_2^+ are quite unique, which provides rich analytical information.

The branching ratios of α-pinene are shown in Figure 6a and 6b. The most abundant ions were: m/z 93 at E/N 60 Td, m/z 42 between 70 and 110 Td, m/z 41 at 120-140 Td, and >150 Td ion m/z 39 was dominant. The dominant contribution of ions m/z 41 and m/z 42 are unique feature among analysed monoterpenes. The molecular ion contribution (m/z 136) has been >1 % and only at low E/N (80 Td).

In previous work with SIFT-MS only ions with m/z 136, m/z 121, m/z 107, m/z 93, m/z 92 and m/z 80 have been observed [14], which is somewhat similar to the major ion contribution at low E/N in this experiment (Figure 6, Table S2).

3-Carene: The branching ratios of 3-carene are shown in Figure 6c and 6d. Ion m/z 93 dominated when E/N was <160 Td, after which the most dominant ion observed was m/z 39. This pattern share similarities only with myrcene. Ions m/z 42 and m/z 41 had similar but much lower contributions compared to α-pinene.

In previous work with SIFT-MS only ions m/z 136, m/z 121, m/z 107, m/z 94, m/z 93, m/z 92 and m/z 80 have been observed [14], which is similar to some major ion contributions at low E/N in this experiment (Figure 6, Table S2).

β-Pinene: The branching ratios of β-pinene are shown in Figure 6e and 6f. Uniquely, ion m/z 93 was the most abundant ion across all E/N, with relative contributions around 60%. The primary ion m/z 136 and ion m/z 69 were steadily decreasing with higher values of E/N, and ion m/z 39 promptly increased after E/N 210 Td. Ion m/z 92 had steady relative contribution around 4 % when E/N was <180 Td, and then suddenly dropped below 1 %.

In previous work with SIFT-MS only ions with m/z 136, m/z 121, m/z 107, m/z 93, m/z 92, m/z 80 and m/z 69 have been observed [14], which is similar to some major ion contributions at low E/N in this experiment (Figure 6, Table S2).

Myrcene: The branching ratios of myrcene are shown in Figure 7a and 7b. The most abundant ion until 150 Td was m/z 93, after which ion m/z 39 started to be dominant. This is a unique pattern shared by 3-carene and myrcene. However, myrcene has a unique presence of m/z 77, which is the second most dominant ion at E/N 170 and 180 Td.

In previous work with SIFT-MS, only ions m/z 136, m/z 121, m/z 94, m/z 93, m/z 92, m/z 80 and m/z 69 have been observed [14], which share some similarity to the major ion contributions at low E/N in this work (Figure 7, Table S2).

Camphene: The branching ratios of camphene are shown in Figure 7c and 7d. At E/N <110 ion m/z 121 was the dominant ion, after which m/z 93 had the highest branching ratio reaching >50% after 210 Td. The presence of ion m/z 121 with the relative ion abundance >30% at lower E/N is a unique feature amongst the analysed monoterpenes.

In previous work with SIFT-MS only ions m/z 136, m/z 121, m/z 108, m/z 107, m/z 93, m/z 92 and m/z 80 have been observed [14], which share some similarity to the major ion contributions at low E/N in this work (Figure 7, Table S2).

R-Limonene: The branching ratios of limonene are shown in Figure 7e and 7f. Ion m/z 93 dominated when E/N was below 170 Td, after which m/z 91 had the highest relative contribution. The unique presence of m/z 91 as the most dominant ion at higher E/N, together with a reasonably high relative abundance of ion m/z 77 makes limonene different from other monoterpenes.

In previous work with SIFT-MS only ions m/z 136, m/z 121, m/z 107, m/z 94, m/z 93, m/z 92, m/z 80 and m/z 68 have been observed [14], which share some similarities to the major ion contributions obtained at low E/N in this work (Figure 7, Table S2).

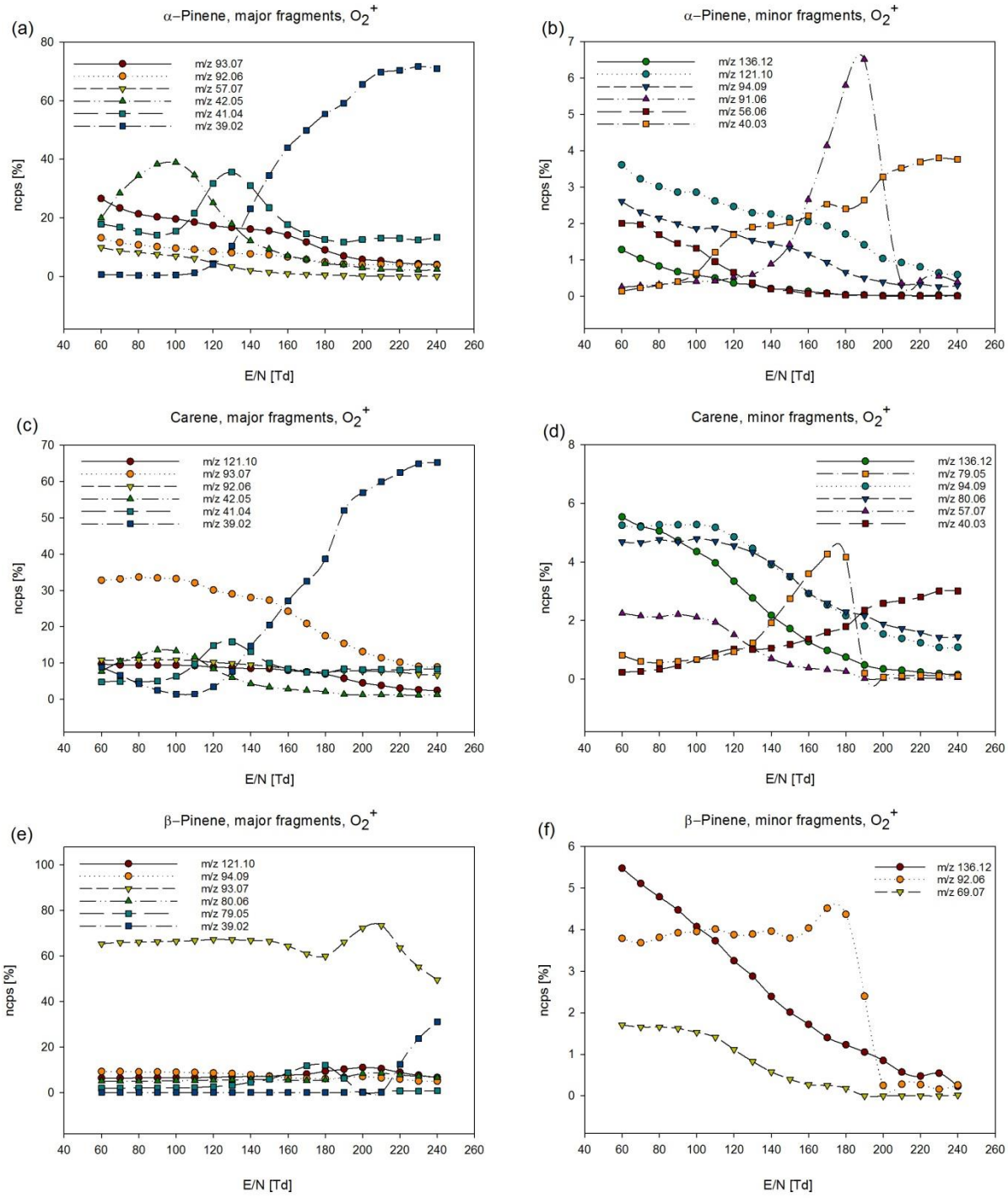

Figure 6. Ion branching of α-pinene, 3-carene and β-pinene using O_2^+ as reagent ion and E/N 60-240 Td. Note that major ions are left and minor ions right.

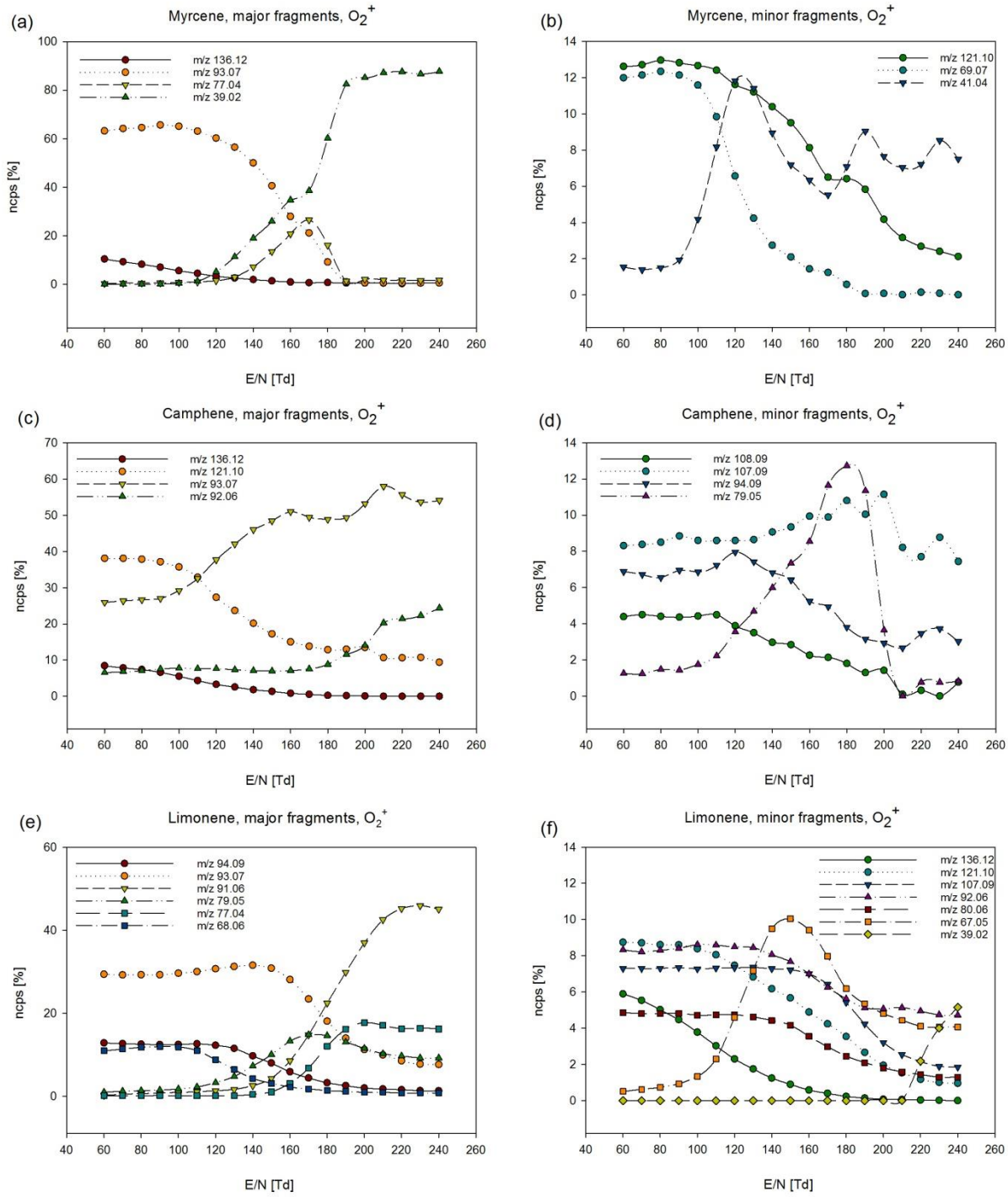

Figure 7. Ion branching of myrcene, camphene and limonene using O_2^+ as reagent ion and E/N 60-240 Td. Note that major ions are left and minor ions right.

Conclusions

SRI-PTR-ToF-MS is a powerful analytical technique that utilizes different ionization modes obtaining high sensitivity together with high, yet unexplored, analytical power. We analysed 6 monoterpenes using a broad E/N range and three ionization modes (H_3O^+, NO^+ and O_2^+). All ionization modes showed a strong dependence of branching ratios when different E/N conditions are applied. Usage of different reagent ions, together with E/N shift, revealed a high number of unique features for each of the analysed monoterpenes. These features have been presented in detail here. The number of unique features observed for each monoterpene suggests the possibility of analysis by this technique to distinguish pure isomers, especially if more energetic chemical ionization is used (such as O_2^+).

These unique properties at certain E/N and ionization mode can be used for compound identification. Given the number of differences observed in this work between different monoterpenes, identification of the pure compounds should not be difficult. For example, based on the unique ion properties of some monoterpenes at certain E/N and ionization mode, an analyst could confirm the presence of some compounds. Using H_3O^+ the presence of myrcene could be confirmed by ion m/z 69 (E/N 100 Td), a fingerprint uniquely present for myrcene amongst the analysed monoterpenes. The presence of 3-carene could be confirmed by ion m/z 136 at low E/N, again uniquely present amongst the analysed monoterpenes. Using NO^+, the ion m/z 119 could be used to confirm 3-carene and myrcene, and only for 3-carene at E/N >180 Td.

These 'fingerprints' could be potentially used in Scots pine research when the chemotypes (trees emitting exclusively either α-pinene, 3-carene or both) need to be separated [21]. The presence of both α- and β-pinene could be confirmed by ion m/z 108 (using NO^+) but there is no obvious unique ion presented in one or another that could be used to distinguish them. However, using results from several E/N and ionization set up together with statistical methods (based on principal component analysis or distance matrix) it might be possible to identify similar compounds (such as α- and β-pinene), and the compounds in a simple monoterpene mixture of two monoterpenes. For example, using O_2^+ ions the branching ratios between each monoterpene are quite different and an algorithm based on scoring the spectra differences (similar to GC-MS identification algorithm) could be used here.

However, more complex monoterpene mixtures (commonly found in some species such as Norway spruce) are not expected to be resolved by this technique. The issues faced when the terpene mix is rich (not just monoterpenes but sesquiterpenes also) is that each key mass in mass spectra that could be used for monoterpene identification could be contaminated from an unknown source (e.g. ion fragment originated from unknown compound), which would compromise the identification. In order to overcome the above mentioned issue fastGC-PTR-ToF-MS would be more adequate method for near to real time monoterpene separation [18].

Acknowledgement

DM and ML gratefully acknowledge the Proton Ionization Molecular Mass Spectrometry (PIMMS) Initial Training Network (ITN), which is funded by the European Commission's 7th Framework Programme under Grant Agreement Number 287382 for financial support, providing a high quality training and the opportunity to link with leaders of cutting edge analytical techniques.

References

[1] J.K. Holopainen, J. Gershenzon, Multiple stress factors and the emission of plant VOCs, Trends Plant Sci. 15 (2010) 176–184. doi:10.1016/j.tplants.2010.01.006.

[2] E. Lewinsohn, T.J. Savage, M. Gijzen, R. Croteau, Simultaneous analysis of monoterpenes and diterpenoids of conifer oleoresin, Phytochem. Anal. 4 (1993) 220–225. doi:10.1002/pca.2800040506.

[3] W. Song, M. Staudt, I. Bourgeois, J. Williams, Laboratory and field measurements of enantiomeric monoterpene emissions as a function of chemotype, light and temperature, Biogeosciences. 11 (2014) 1435–1447. doi:10.5194/bg-11-1435-2014.

[4] N. Yassaa, J. Williams, Enantiomeric monoterpene emissions from natural and damaged Scots pine in a boreal coniferous forest measured using solid-phase microextraction and gas chromatography/mass spectrometry, J. Chromatogr. A. 1141 (2007) 138–144. doi:10.1016/j.chroma.2006.12.006.

[5] F. Biasioli, F. Gasperi, C. Yeretzian, T.D. Märk, PTR-MS monitoring of VOCs and BVOCs in food science and technology, TrAC Trends Anal. Chem. 30 (2011) 968–977. doi:10.1016/j.trac.2011.03.009.

[6] R. Fernández del Río, M.E. O'Hara, A. Holt, P. Pemberton, T. Shah, T. Whitehouse, C.A. Mayhew, Volatile Biomarkers in Breath Associated With Liver Cirrhosis — Comparisons of Pre- and Post-liver Transplant Breath Samples, EBioMedicine. 2 (2015) 1243–1250. doi:10.1016/j.ebiom.2015.07.027.

[7] J. Peñuelas, M. Staudt, BVOCs and global change, Trends Plant Sci. 15 (2010) 133–144. doi:10.1016/j.tplants.2009.12.005.

[8] J.S. Yuan, S.J. Himanen, J.K. Holopainen, F. Chen, C.N. Stewart Jr, Smelling global climate change: mitigation of function for plant volatile organic compounds, Trends Ecol. Evol. 24 (2009) 323–331. doi:10.1016/j.tree.2009.01.012.

[9] D. Materić, D. Bruhn, C. Turner, G. Morgan, N. Mason, V. Gauci, Methods in Plant Foliar Volatile Organic Compounds Research, Appl. Plant Sci. 3 (2015) 1500044. doi:10.3732/apps.1500044.

[10] R.S. Blake, P.S. Monks, A.M. Ellis, Proton-Transfer Reaction Mass Spectrometry, Chem. Rev. 109 (2009) 861–896. doi:10.1021/cr800364q.

[11] A.M. Ellis, C.A. Mayhew, Proton Transfer Reaction Mass Spectrometry: Principles and Applications, 1 edition, Wiley-Blackwell, Chichester, West Sussex, 2014.

[12] D. Smith, P. Španěl, Selected ion flow tube mass spectrometry (SIFT-MS) for on-line trace gas analysis, Mass Spectrom. Rev. 24 (2005) 661–700. doi:10.1002/mas.20033.

[13] P.K. Misztal, M.R. Heal, E. Nemitz, J.N. Cape, Development of PTR-MS selectivity for structural isomers: Monoterpenes as a case study, Int. J. Mass Spectrom. 310 (2012) 10–19. doi:10.1016/j.ijms.2011.11.001.

[14] T. Wang, P. Španěl, D. Smith, Selected ion flow tube, SIFT, studies of the reactions of H3O+, NO+ and O2+ with eleven C10H16 monoterpenes, Int. J. Mass Spectrom. 228 (2003) 117–126. doi:10.1016/S1387-3806(03)00271-9.

[15] A. Tani, S. Hayward, C.N. Hewitt, Measurement of monoterpenes and related compounds by proton transfer reaction-mass spectrometry (PTR-MS), Int. J. Mass Spectrom. 223–224 (2003) 561–578. doi:10.1016/S1387-3806(02)00880-1.

[16] A. Jordan, S. Haidacher, G. Hanel, E. Hartungen, J. Herbig, L. Märk, R. Schottkowsky, H. Seehauser, P. Sulzer, T.D. Märk, An online ultra-high sensitivity Proton-transfer-reaction mass-spectrometer combined with switchable reagent ion capability (PTR + SRI − MS), Int. J. Mass Spectrom. 286 (2009) 32–38. doi:10.1016/j.ijms.2009.06.006.

[17] S.D. Maleknia, T.L. Bell, M.A. Adams, PTR-MS analysis of reference and plant-emitted volatile organic compounds, Int. J. Mass Spectrom. 262 (2007) 203–210. doi:10.1016/j.ijms.2006.11.010.

[18] D. Materić, M. Lanza, P. Sulzer, J. Herbig, D. Bruhn, C. Turner, N. Mason, V. Gauci, Monoterpene separation by coupling proton transfer reaction time-of-flight mass spectrometry with fastGC, Anal. Bioanal. Chem. 407 (2015) 7757–7763. doi:10.1007/s00216-015-8942-5.

[19] M. Lanza, W.J. Acton, S. Jürschik, P. Sulzer, K. Breiev, A. Jordan, E. Hartungen, G. Hanel, L. Märk, C.A. Mayhew, T.D. Märk, Distinguishing two isomeric mephedrone substitutes with selective reagent ionisation mass spectrometry (SRI-MS), J. Mass Spectrom. 48 (2013) 1015–1018. doi:10.1002/jms.3253.

[20] A. Tani, S. Hayward, A. Hansel, C.N. Hewitt, Effect of water vapour pressure on monoterpene measurements using proton transfer reaction-mass spectrometry (PTR-MS), Int. J. Mass Spectrom. 239 (2004) 161–169. doi:10.1016/j.ijms.2004.07.020.

[21] J. Bäck, J. Aalto, M. Henriksson, H. Hakola, Q. He, M. Boy, Chemodiversity of a Scots pine stand and implications for terpene air concentrations, Biogeosciences. 9 (2012) 689–702. doi:10.5194/bg-9-689-2012.

[22] T. Räisänen, A. Ryyppö, S. Kellomäki, Monoterpene emission of a boreal Scots pine (Pinus sylvestris L.) forest, Agric. For. Meteorol. 149 (2009) 808–819. doi:10.1016/j.agrformet.2008.11.001.